LASERLAB-EUROPE

The Integrated Initiative of European Laser Research Infrastructures III

Grant Agreement number: 284464

WT:3 – Laser and Photonics for Biology and Health (BIOPTICHAL)

Deliverable number: 30.14

Report on optical tools and methodologies for the study, diagnosis and therapy of human diseases

Lead Beneficiary: 1

Due date: Month 42

Date of delivery: Month 43

Project webpage: www.laserlab-europe.eu

Deliverable Nature	
R = Report, P = Prototype, D = Demonstrator, O = Other	R
Dissemination Level	
PU = Public PP = Restricted to other programme participants (incl. the Commission Services) RE = Restricted to a group specified by the consortium (incl. the Commission Services) CO = Confidential, only for members of the consortium (incl. the Commission Services)	PU

A. Abstract / Executive Summary

During the project, several participants have worked toward improved optical diagnostic tools both to provide better guidance in diagnosing disease, but also to guide therapy.

High spatio-temporally resolved microscopy. Imaging technologies have driven outstanding progress in the comprehension of the workings of biological systems. However, the main shortcoming of available technologies is their incapability of imaging multiple fast phenomena with adequate spatio-temporal resolution. In this work, we combined the advantages of multi-photon microscopy with a random access excitation scheme to realize a new microscope (RAMP) capable of optically recording fast physiological events occurring in a wide-field of view. The RAMP microscope, in combination with a new generation of fluorinated voltage sensitive dye and calcium indicator, was used to simultaneously record electrical activity from clusters of Purkinje cells in acute cerebellar slices and monitoring action potential propagation and calcium release in cardiac cells from pathological settings. These results show the strength of this technique in describing the temporal dynamics of neuronal assemblies and providing fundamental insights in cardiac pathology.

Skin cancer diagnosed with multiphoton microscopy. LENS will also exploit a combination of non-linear microscopy techniques (TPE, SHG, FLIM, SLIM) to the diagnosis of skin cancer in vivo, which will be tested on volunteers in the dermatologic clinic Villa S. Chiara, Dept. of Dermatology, Univ. of Florence.

Skin cancer diagnosed with fluorescence lifetimes and photobleaching rates. The main focus of this subtask has been to assess the possibility and potential of a combined time-resolved fluorescence spectroscopy method including parallel analysis of tissue autofluorescence (AF) lifetimes and photo-bleaching rates. Results show they provide complementary sets of diagnostic information.

Diffuse reflectance/fluorescence system for assessment of tissue optical properties. A system for absolute assessment of the tissue optical properties and a fluorophore concentration in tissue is developed. The system is based on low-cost LEDs as a light-source unit and avalanche photodiodes filtered for different light detection wavelenghts in the detection unit. The deetection unit further consist os dichroic mirrors and optical bandpass filters. By sequentially turning on the sources, one at a time, both diffuse reflectance ad induced fluorescence can be detected. The results from measurement on 169 different optical tissue phantoms show that the tissue absorption can be determined with an accuracy of 5%, the tissue scattering with 2% and the fluorophore concentration with 8%, limited by the obtained signal-to-noise ratio (2 s recording for one wavelength set of data).

Gas in scattering media absorption spectroscopy (GASMAS) for assessing lung function of premature babies. Within the project the GASMAS technique has been refined in collaboration between LU, LENS and POLIMI. The biomedical application has been expanded, and a major part of the work has been directed towards develop a technique to non-invasively assess lung function in premature babies. A first clinical evaluation study has been conducted, and it has been possible to measure the oxygen signal of interest in all babies included in the study. The results indicate that the sensitivity of the technique has to be further improved to gain real clinical interest, and a Eurostars project has been started with this objective.

B. Deliverable Report

1 Introduction

High spatio-temporally resolved microscopy. Most approaches to the optical recording of fast physiological processes in excitable cells rely on one-photon methods. Although these methods can be used to generate high signal-to-noise ratio, in intact tissue their effectiveness is markedly limited. In order to record physiological processes in intact systems maintaining a high spatial resolution, nonlinear optical methods, such as multi-photon

fluorescence microscopy are needed [1,2]. In this regard, the major limiting factor of non-linear microscopes is their scanning time. For this reason, the optical recording is possible only in a single position by using a line scanning procedure [3,4]. In principle, the optical measurement of time-dependent processes does not require the production of images at all. Instead, more time should be spent collecting as many photons as possible from selective positions. Using this approach, fast physiological processes, like APs in the soma of multiple neurons, can be recorded at a sampling frequency of more than 1 kHz. This cannot be achieved with a standard galvanometer mirror since about 1 ms is the time required to reach and stabilize a new position. On the other hand, scanning a set of points within a plane at high speed is possible with two orthogonal acousto-optic deflectors.

Skin cancer. Non-linear optical (NLO) microscopy offers promising solutions for both in vivo and ex vivo tissue imaging at sub-cellular level and it can provide both morphological and functional information in a label-free modality. The combination of NLO microscopy techniques providing morphological information, together with those providing functional information is a crucial issue for tissue classification and pathological assessment.

Workstation fluorescence lifetimes and fluorescence bleaching rates. There exists a need to improve diagnostic imaging. Combining fluorescence lifetimes and bleaching rates may provide more diagnostic information than any of the techniques alone.

Diffuse reflectance/fluorescence system for assessment of tissue optical properties. There is a need the tissue optical properties and the photosensitiser concentration in planning the dosimetry for photodynamic thereapy. There is a lack of systems to conduct such measurements. It would thereby be welcome to obtain a compact, low-cost system for such purpose, also meeting the clinical requirements. These requirements include sterilisability of the measurement probe head, and to cope witht he examination room light conditions. The presented system fulfills these conditions.

Gas in scattering media absorption spectroscopy (GASMAS) for assessing lung function of premature babies. It has previously been demonstrated that the GASMAS technique enable to measure gas constituents in highly scattering media. Biomedical applications have been for measuring the gas content in sinus cavities as a diagnostic tool for sinusitis. It has been challenging to measure absolute concentrations of the oxygen, as the technique only provide the optical density, i.e. the absorption times the path length of the light through the gas. Simultaeous measurements of water vapour, has been employed as a means for calibration, as that concentration is known. The remaining challenge is though that the attenuation of the light for the oxygen and water vapour wavelengths differ, causing errors in this relative measurements.

Objectives

High spatio-temporally resolved microscopy. In this work we develop an ultrafast random access multi-photon microscope (RAMP) bases on acousto-optic deflectors that, in combination with voltage-sensitive dyes and calcium indicator, is used to simultaneously measure action potentials and calcium release at multiple sites with sub-millisecond temporal and sub-micrometre spatial resolution in real time.

Skin cancer. The designed study aimed at using multimodal multiphoton microscopy and spectroscopy for in vivo early diagnosis of skin cancer.

Workstation fluorescence lifetimes and fluorescence bleaching rates. The aim has been to construct a workstation for combined fluorescence lifetime and photobleaching rates as well as to evaluate such a system on tissue measurements.

Diffuse reflectance/fluorescence system for assessment of tissue optical properties. The objective was to develop a compact, low-cost system to assess the optical properties of tissue as well as the concentration of a PDT photosensitizer. The results should be

insensitive to the room light conditions and provide an accuracy of better than 10% of all properties.

Gas in scattering media absorption spectroscopy for assessing lung function of premature babies. This project concerns developing an instrument to be able to measure the oxygen concentration in the air in the lungs of premature babies. The technique employed is GASMAS. The difficulties have been to firstly at all detect the very weak signals from the gas absorption from the lung volume, and secondly to use the measured signal to extract the oxygen concentration in the gas contained in the lung.

2 Work performed / results / description

High spatio-temporally resolved microscopy. The basic design of our RAMP imaging system is show in figure 1A. The excitation was provided by a high-power, passively mode-locked fiber laser operating in the 1064 nm spectral range. The scanning head was developed by using an acousto-optical deflection (AOD) system composed of two AODs crossed at 90°. To compensate for the larger dispersion due to two crossed AODs, we used an acousto-optic modulator placed at 45° with respect to the two axes of the AODs. The fluorescence signal was collected in backward direction by the excitation objective and in forward direction using a high numerical aperture condenser lens. For each detection direction, a dichroic mirror was used to split the two spectral components of the fluorescence signal, the red and the green emission light. The fluorescence signal was detected by two independent photon-counting modules based on the GaAsP photomultiplier tube (PMT). The RAMP microscope is capable of commutating between two positions of the focal plane in ~4 µs. In a typical measurement, we probed 5–10 different sites. The length of the scanned lines ranged from 2 to 10 µm with integration time per membrane pass ~100 µs, leading to a temporal resolution on the order of 0.5–1 ms.

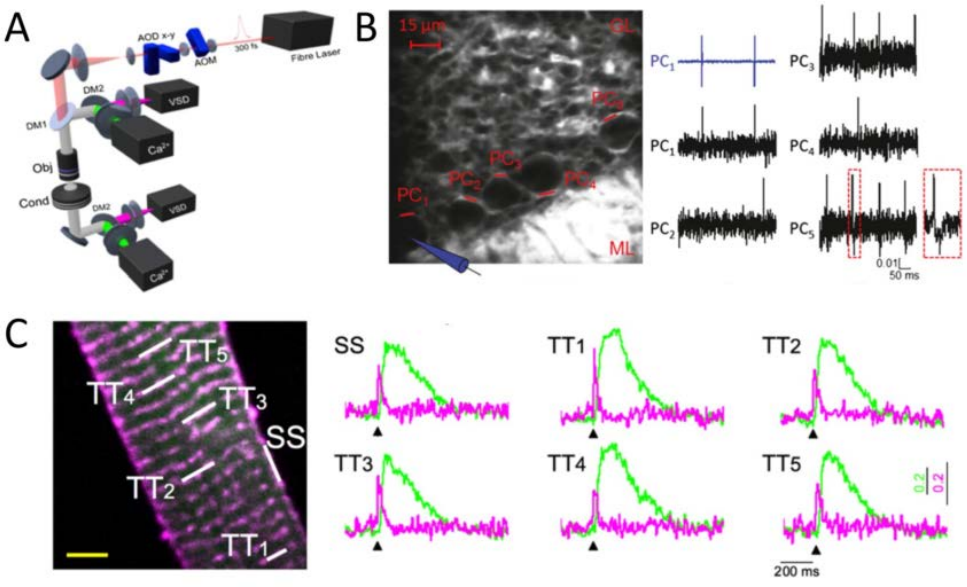

Fig. 1 RAMP imaging system.

RAMP microscope was used to record action potential simultaneously from clusters of Purkinje cells in acute cerebellar slices. This recording was achieved by rapidly positioning the laser excitation with an acousto-optic modulator to sample a patch of membrane from each cell in <100 µs; for recording from five cells as in Figure 1B, multiplexing permits a temporal resolution of ~400 µs sufficient to capture every spike. The same methodology was also used to record of action potential and Ca^{2+} transients in an isolated cardiomyocyte. In this case, RAMP is used to simultaneously excite both dyes while band-pass filters are used

to select the two distinct spectral ranges of the fluorescence emission spectra. A spectral unmixing procedure was applied to properly uncouple the Ca^{2+} and the voltage signals. Figure 1C is an example of real-time simultaneous optical recording from six different membrane areas located at the surface sarcolemma (SS) and in five different T-tubules (TTi). The signal-to-noise ratio is sufficient to detect the presence of an action potential (magenta traces) occurring at sarcolemma and to assess the temporal features of the Ca^{2+} transient (green traces) in the surrounding cytoplasm. We found that the tight electrical coupling between different sarcolemmal domains is guaranteed only in healthy cardiomyocytes. In fact, we found that intracellular action potential propagation in various pathologically settings frequently fails and may be followed by local spontaneous electrical activity [5]. Sites where T-tubules fail to conduct action potential showed a slower and reduced local Ca^{2+} transient compared with regions with electrically coupled elements. Moreover, we found that spontaneous depolarization events occurring in failing T-tubules can trigger local Ca^{2+} release, resulting in Ca^{2+} sparks [6]. The occurrence of tubule-driven depolarizations and Ca^{2+} sparks may contribute to the arrhythmic burden in pathologic hearth.

Skin cancer – in vivo. During the period we are reporting about, we built a custom multimodal multiphoton microscope inside a research lab located in the dermatological clinic of the University of Florence (Azienda Ospedaliera Firenze Centro – c/o Villa Santa Chiara). In addition, we prepared the Clinical Protocol to be submitted to the Local Ethical Committee for in vivo studies.

Unfortunately, due to the regional spending review policy on health assistance, related to the current economic crisis, the Dermatological Clinic has moved in another building and the spaces dedicated to the clinical dermatological activities have been drastically reduced, making impossible to have a research lab dedicated to clinical investigation with new optical devices in the new location. For this reason, the developed devices have been moved to Lens, limiting the research activity to be carried out to ex vivo tissues.

Our new plan is to perform research activity on ex vivo fixed tissue slices of various biological tissues (not only skin), instead of in vivo on living subject, using the same optical methods. The activity could be turned again to in vivo investigation in the future, provided that a proper location for the experimental setup is found within the dermatological hospital.

Skin cancer – ex vivo. During the period we are reporting about, we performed imaging of various ex vivo tissue samples using multimodal non-linear microscopy. In particular, we focused our attention on both cancerous and non-cancerous (atherosclerosis) diseases using both thin slices and fresh massive biopsies of tissues.

For cancerous lesions, samples of healthy colon mucosa were examined and compared to both adenomatous and adenocarcinoma tissues. Images acquired using TPF microscopy on fresh colon biopsies demonstrated good correlation with conventional histological examination carried out on the same samples. A quantitative morphological analysis classified tissues on the basis of both nucleus-to-cytoplasm ratio and cellular asymmetry. Functional characterization, performed by comparing the relative intensities of NADH and FAD fluorescence, demonstrated an altered metabolic activity in both adenomatous polyp and adenocarcinoma compared to healthy mucosa. In particular, adenomatous tissue showed a metabolic activity more similar to adenocarcinoma than to healthy mucosa.

For non-cancerous lesions, we demonstrated that SHG microscopy can be used to image both cholesterol and collagen and to discriminate the two molecules by means of a detailed analysis of the detected SHG signal. In particular, we first provided a demonstration of the potential of SHG for imaging cholesterol deposition within atherosclerotic plaques. Then we focus the attention on forward and backward scattered SHG microscopy, demonstrating that the simultaneous detection of forward and backward scattered SHG signal can be successfully used for discriminating cholesterol deposition from connective tissue in the arterial wall. Finally, image pattern analysis methods were implemented and used for scoring collagen organization in plaques against normal arterial wall, finding altered collagen

architecture within plaques. The used methods allowed quantitatively determining collagen fibres anisotropy, size, and spacing in both atherosclerotic depositions and normal arterial wall.

Workstation fluorescence lifetimes and fluorescence bleaching rates. An experimental workstation for parallel imaging of skin AF lifetimes and photo-bleaching rates was assembled (Fig.2). The setup comprises a pico-second excitation lasers (PicoQuant: pulse half-width 59 ps, 405nm/472nm/510nm, mod. LDH-D-C-405/472/510) laser controller, monochromator, photon counting detector with temporal resolution of 180ps (mod. Becker&Hickl, PMC100-4), data processing system "time-correlated single photon counting" with time resolution 6.6 ps, (TCSPC, mod. Becker&Hickl SPC-150), Y-type optical fiber and a scanning system. Skin AF decay distributions were periodically collected over a fixed period of the time.

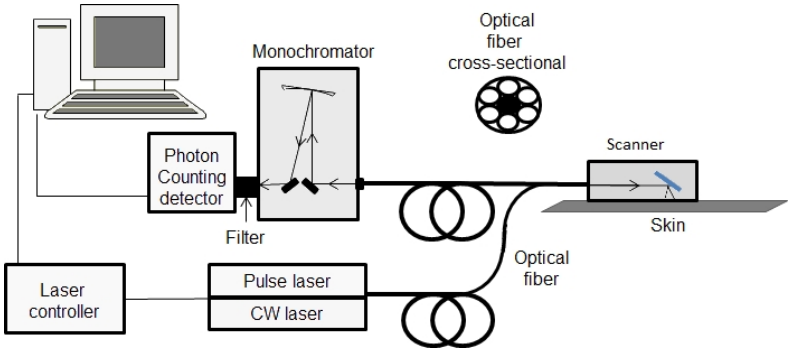

Fig. 2 Workstation for parallel imaging of tissue FLT and photo-bleaching rates.

Each measurement contained a temporal distribution of AF decay and a number of collected photons acquired during the each measurement. Typical collection time for one measurement was ~10 seconds. Due to the AF photo-bleaching process, the number of collected photons for each subsequent measurement decreases, thereby giving the opportunity to obtain the AF photo-bleaching rates for each single pixel. The photo-bleaching rates were defined according to expression (1).

$$N(G) = (M_{t0}[G]-M_t[G])/M_{t0}[G] \quad (1);$$

Where N(G) matrix represents normalized AF intensity decrease for each pixel during the excitation period t, $M_{t0}[G]$ – photon counts matrix at the excitation start moment, $M_t[G]$ – photon counts matrix after fixed time period (for example 1 min.) of CW excitation and G – time gate of the fluorescence decay distribution.

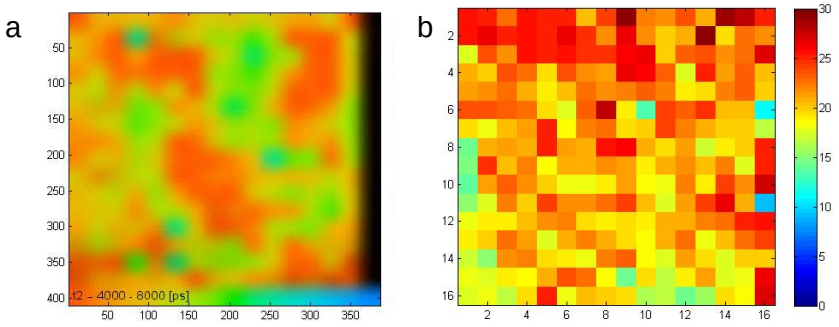

Fig. 3 Healthy skin τ_2 distribution image (a) and corresponding photo-bleaching rate image (b) after 3 minutes of 405 nm pulse excitation. The photo-bleaching rates were obtained at 5 – 45 ns time gate.

Figure 3 represents lifetime component τ_2 distribution image and corresponding photo-bleaching rate distribution image. Photo-bleaching distribution image demonstrates AF intensity decreasing after 3 minutes of 405 nm CW excitation with mean power density ~40mW/cm^2.

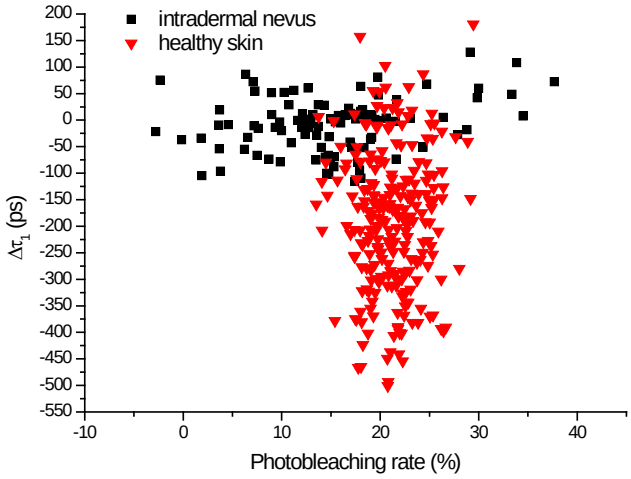

Fig.3. Correlation graph of photo-bleaching rate and shift of the lifetime component τ_1 during the 3 minutes of 405 nm pulse excitation with mean power density ~40 mW/cm^2.

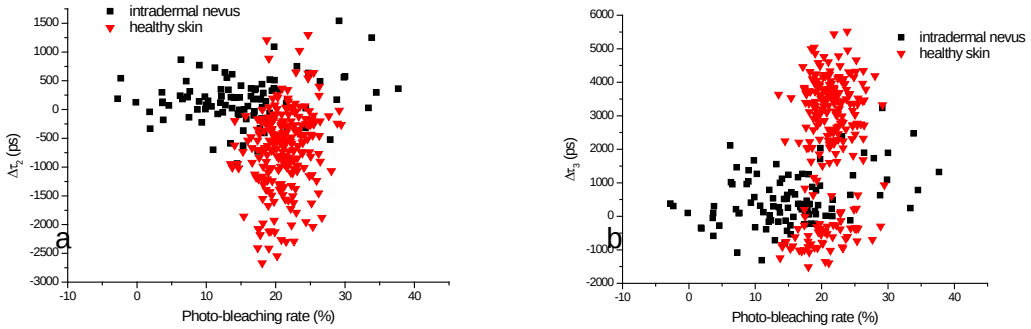

Fig.4. Correlation graphs of photo-bleaching rate and shift of the lifetime component during the 3 minutes of 405 nm CW excitation with mean power density ~40mW/cm^2: (a) photo-bleaching rate and shifts of the lifetime component τ_2, (b) photo-bleaching rate and shifts of the lifetime component τ_3.

In-vivo skin can be characterized by two dynamic parameters autofluorescence lifetime and photo-bleaching rate. Figure 3 and 4 represent correlations graphs between photo-bleaching rates and shifts of the AF lifetime components during the 3 minutes of 405 nm pulse excitation. The lifetime shifts were defined as a difference of τ values at excitation start moment and after 3 minutes. The values of photo-bleaching rates and AF lifetimes components were extracted from the 16x16 matrixes of healthy skin and intradermal nevus. The healthy skin is characterized by AF intensity decreasing of ~20% on its initial value and significant changes of AF lifetime components $\tau_{1,2,3}$. While the lifetime components $\tau_{1,2,3}$ obtained from intradermal nevus demonstrates relatively insignificant changes during the photo-bleaching process.

Design of prototype device for non-invasive quantitative skin diagnostics. The prototype device consists of Pico second laser, photon detector, TCSPC system, laser and scanner controller, scanner, and PC with touch screen display, see Fig. 5. The TCSPS system is managed by the touch screen display. The box size is 400mm x 400mm x 200mm with display on the top and scanner`s box inside. The scanner connects with laser and photon detector by optical fiber and it can be moved in necessary direction.

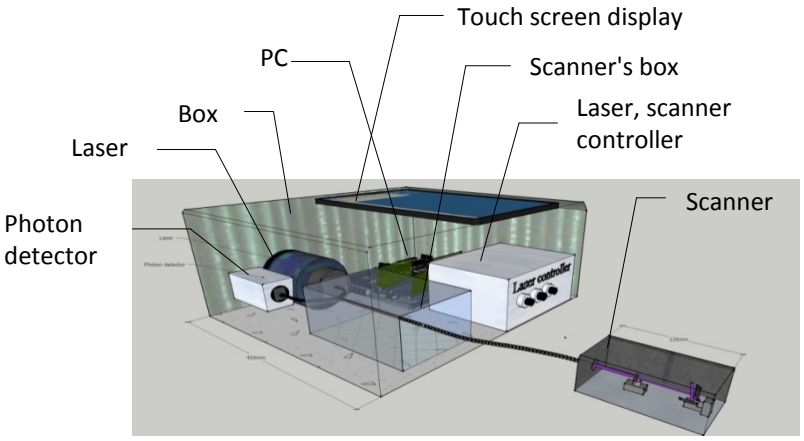

Fig. 5 Design of prototype device for parallel imaging of tissue FLT and photo-bleaching rates.

Diffuse reflectance/fluorescence system for assessment of tissue optical properties. A diffuse reflectance/fluorescence system was developed. The outline of the system is presented in Fig. 6. It is based on five light sources (LEDs at 375, 405, 530, 635 nm and one white) as well as five detectors (a PD filtered at 405 nm, and APDs filtered at 470, 530 635 and 690 nm, respectively). The system runs a set of all sources in sequence plus a period with all sources off (for background measurements) at a repetition frequency of 777 Hz.

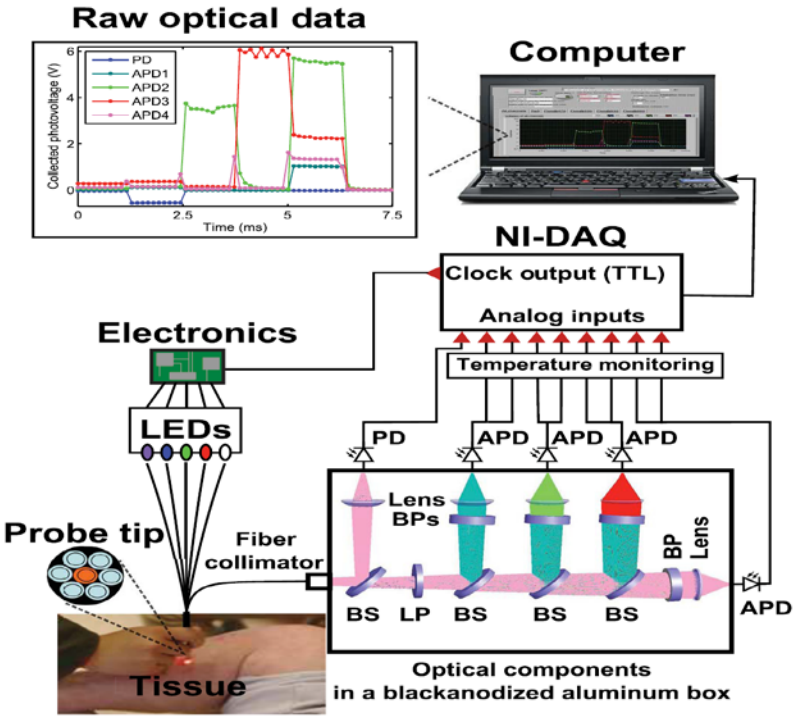

Fig. 6 Schematic illustration of duffuse reflectance/fluorescence system developed.

The performance of the system was evaluated on a series of 169 tissue phantoms, with absorption, scattering and fluorophore concentration properties varying. About half the set, chosen to be representative of all scattering, absorption and fluorophore values, was used as a training set for multivariate analysis, while the remaining phantoms were used to predict the prediction accuracy. The multivariate technique employed was Support Vector Machines. The results of the evaluation are presented in Fig. 7.

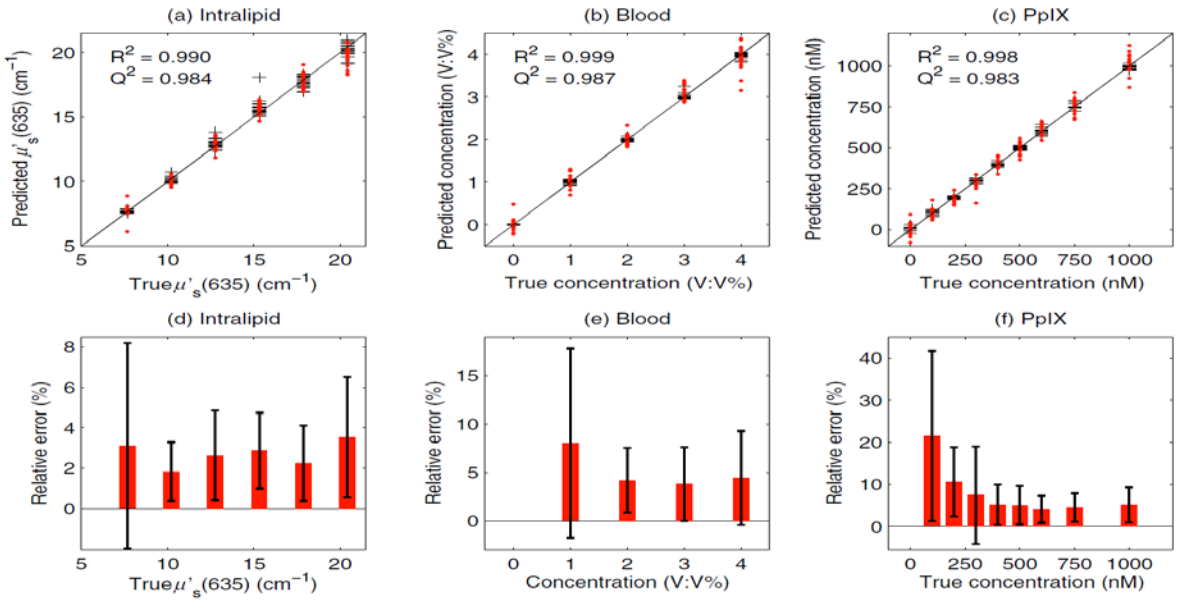

Fig. 7 (a–c) PpIX quantification in intralipid blood phantoms with various optical properties using Least squares support vector machines regression with twofold cross-validation (135 samples for training and 134 samples for validation). The dark solid lines indicate the diagonal of best prediction (coordinates 1:1). R2 and Q2 are the correlation coefficients between the true parameter and model response for training and validation, respectively. (d–f) Relative error of the predicted parameters (mean ± SD). The data have not been temperature calibrated because of a long waiting time of ~4 h prior to measurement. Schematic illustration of duffuse reflectance/fluorescence system developed.

Gas in scattering media absorption spectroscopy for assessing lung function of premature babies. A compact system for clinical GASMAS measurements has been developed and has been evaluated in *in vivo* measurements, first in a proof-of-concept study, and later in a clinical study. The measurement arrangement is illustrated in Fig. 8.

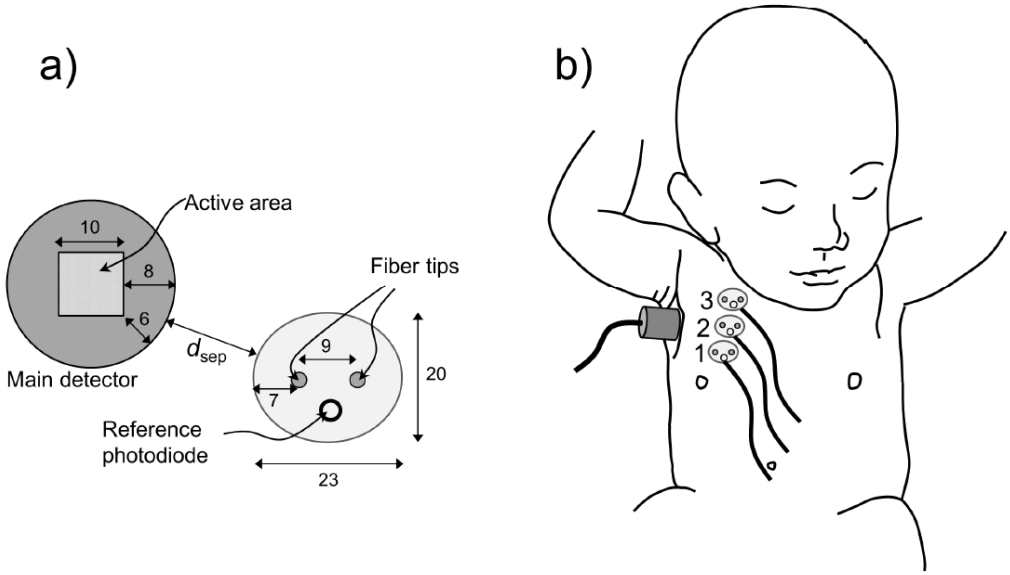

Figure 8. a) Schematic drawing of the measurement probes, illustrating their dimensions (in mm) and their relative positions during the measurements. b) Schematic illustration of bilateral spectroscopic measurements of intrapulmonary gas contents in neonatal infants. Light emitted (dark grey dots) at mid-collar level just above the nipple (1), between the nipple and the collar bone (2) and just below the collar bone (3), was detected (grey cylinder) in the armpit or slightly below on the same side.

Laser spectroscopy has been used to measure contents of oxygen gas (at 760 nm) and of water vapor (at 935 nm) in the lungs of 29 healthy newborn full-term infants (birth weight 2900-3900 g). The skin above the lungs was illuminated using two low-power diode lasers, and diffusely emerging light was detected with a photodiode. Of the total 390 lung measurements performed, clear detection of oxygen gas was recorded in 60%, defined by signal-to-noise ratios >3. In all 29 infants, oxygen was detected. Probe and detector positions for optimal pulmonary gas detection were determined. There were no differences in signal quality with respect to gender, body side or body weight.

3 Conclusions

High spatio-temporally resolved microscopy. In conclusion, here we develop a new optical method capable of optically recording fast physiological events occurring in a wide-field of view. The system was applied to simultaneously record electrical activity from clusters of Purkinje cells in acute cerebellar slices and monitoring action potential propagation and calcium release in cardiac cells from pathological settings.

Skin cancer. The morpho-functional analysis carried out on ex vivo tissues using multimodal non-linear microscopy may represent a powerful tool for early diagnosis of tumors and may also be extended to the diagnostics of other tissues. In addition, the methods represent a support, or also a competitive label-free diagnostic alternative to standard histopathological methods for evaluating biological tissues. Further, the methods developed could be translated to in vivo diagnostics, once the in vivo imaging facility will be restored.

Workstation fluorescence lifetimes and fluorescence bleaching rates. Correlations between FLT and PBR determined in-vitro and in-vivo will be exploited to design a prototype device for non-invasive quantitative skin diagnostics. A new system is now under design and development.

Diffuse reflectance/fluorescence system for assessment of tissue optical properties. The compact system was providing results well meeting the requirements in terms of accuracy. It was also insensitive to background light as a result of the lock-in like detection scheme, where the background was measured and subtracted in every measurement cycle.

Gas in scattering media absorption spectroscopy for assessing lung function of premature babies. The ability to measure pulmonary oxygen content in healthy full-term neonates with this technique suggests that with further development the method might be implemented in clinical practice for lung monitoring in neonatal intensive care. As an outcome of these studies, such a development is now ongoing, supported through the Eurostars programme.

4 References

1. F. Helmchen and W. Denk, “Deep tissue two-photon microscopy,” Nat. Methods 2, 932-940 (2005).
2. W. R. Zipfel, R. M. Williams, and W. W. Webb, “Nonlinear magic: multiphoton microscopy in the biosciences” Nat. Biotechnol. 21, 1369-1377 (2003).
3. D. A. Dombeck, M. Blanchard-Desce, and W. W. Webb, “Optical recording of action potentials with second-harmonic generation microscopy,” J. Neurosci. 24, 999-1003 (2004).
4. L. Sacconi, D. A. Dombeck, and W. W. Webb, “Overcoming photodamage in second-harmonic generation microscopy: real-time optical recording of neuronal action potentials,” Proc. Natl. Acad. Sci. U S A 103, 3124-3129 (2006).
5. L. Sacconi, C. Ferrantini, J. Lotti, R. Coppini, P. Yan, L. M. Loew, C. Tesi, E. Cerbai, C. Poggesi, F. S. Pavone, Action potential propagation in transverse-axial tubular system is impaired in heart failure, Proc Natl Acad Sci U S A, 109 5815–5819 (2012).
6. C. Crocini, R. Coppini, C. Ferrantini, P. Yan, L. M. Loew, C. Tesi, E. Cerbai, C. Poggesi, F. S. Pavone, L. Sacconi, Defects in T-tubular electrical activity underlie local alterations of calcium release in heart failure. Proc Natl Acad Sci U S A, 111 15196-15201 (2014).

5 Papers

- L. Sacconi, C. Ferrantini, J. Lotti, R. Coppini, P. Yan, L. M. Loew, C. Tesi, E. Cerbai, C. Poggesi, F. S. Pavone, Action potential propagation in transverse-axial tubular system is impaired in heart failure, Proc Natl Acad Sci U S A, vol. 109 pp. 5815–5819 (2012). doi: 10.1073/pnas.1120188109.
- P. Yan, C. Acker, WL. Zhou, P. Lee, C. Bollensdorff, A. Negrean, J. Lotti, L. Sacconi, S. D. Antic, P. Kohl, H. D. Mansvelder, F. S. Pavone, and L. M. Loew, Palette of fluorinated voltage sensitive hemicyanine dyes, Proc Natl Acad Sci U S A, vol. 109 pp. 20443–20448 (2102). doi: 10.1073/pnas.1214850109.
- L. Silvestri, A. L. Allegra Mascaro, J. Lotti, L. Sacconi, F. S. Pavone, Advanced optical techniques to explore brain structure and function, JIOHS, vol. 6, pp. 1230002-15 (2013). doi: 10.1142/S1793545812300029.
- A. L. Allegra Mascaro, L. Silvestri, L. Sacconi, F. S. Pavone, Non-linear laser imaging for neuroscience, IEEE Photonics Journal, vol. 5, pp 0701006 (2013). doi: 10.1109/JPHOT.2013.2250941.
- C. Ferrantini, C. Crocini, R. Coppini, F. Vanzi, C. Tesi, E. Cerbai, C. Poggesi, F. S. Pavone, L. Sacconi, The transverse-axial tubular system of cardiomyocytes, Cell. Mol. Life Sci., vol. 70 pp 4695-4710 (2013). doi: 10.1007/s00018-013-1410-5.
- C. Crocini, R. Coppini, C. Ferrantini, P. Yan, L. M. Loew, C. Tesi, E. Cerbai, C. Poggesi, F. S. Pavone, L. Sacconi, Defects in T-tubular electrical activity underlie local alterations of calcium release in heart failure. Proc Natl Acad Sci U S A, vol. 42 pp. 15196-15201 (2014). doi: 10.1073/pnas.1411557111.
- C. Crocini, R. Coppini, C. Ferrantini, F. S. Pavone, L. Sacconi, Functional cardiac imaging by random access microscopy. Front. Physiol., vol. 5 (2014). doi: 10.3389/fphys.2014.00403.
- D. Kapsokalyvas, N. Bruscino, D. Alfieri, V. de Giorgi, G. Cannarozzo, R. Cicchi, D. Massi, N. Pimpinelli, and F. S. Pavone, *Spectral morphological analysis of skin lesions with a polarization multispectral dermoscope*, Opt. Express **21**, 4826-4840 (2013)
- R. Cicchi, A. Sturiale, G. Nesi, D. Kapsokalyvas, G. Alemanno, F. Tonelli, and F.S. Pavone, *Multiphoton morpho-functional imaging of healthy colon mucosa, adenomatous polyp and adenocarcinoma*, Biomed. Opt. Express **4**, 1204-1213 (2013) **DOI** 10.1364/BOE.4.001204
- R. Cicchi, A. Cosci, S. Rossari, D. Kapsokalyvas, E. Baria, V. Maio, D. Massi, V. De Giorgi, N. Pimpinelli, and F. S. Pavone, *Combined fluorescence-Raman spectroscopic setup for the diagnosis of melanocytic lesions*, J. Biophoton. **7**, 86-95 (2014) **DOI** 10.1002/jbio.201200230 (2013)
- R. Cicchi, C. Matthäus, T. Meyer, A. Lattermann, B. Dietzek, B. R. Brehm, J. Popp, and F. S. Pavone, *Characterization of collagen and cholesterol deposition in atherosclerotic arterial tissue using non-linear microscopy*, J. Biophoton. **7**, 135-143 (2014) **DOI** 10.1002/jbio.201300055 (2013)
- R. Cicchi, and F. S. Pavone, Multimodal nonlinear microscopy: a powerful label-free method for supporting standard diagnostics on biological tissues, J. Innov. Opt. Health Sci. 7, 1330008 (2014) DOI 10.1142/S1793545813300085
- I.Ferulova, A.Lihachev, J.Spigulis. Photobleaching effects on in-vivo skin autofluorescence lifetime. J.Biomed.Opt., 20(5), 051031 (2015).
- A.Lihachev, I.Ferulova,.J.Spigulis, D.Chorvat. Parallel measurements of in-vivo skin autofluorescence lifetimes and photobleaching rates. IFMBE Proc. 48, 78-81 (2014).
- A. Lihachev, I. Ferulova, K. Vasiljeva, J. Spigulis. Investigation of in-vivo skin autofluorescence lifetimes under long-term cw optical excitation. Quant.Electr., 44 (8), 770-773 (2014).
- H Xie, Z Xie, M Mousavi, N Bendsoe, M Brydegaard, J Axelsson, Stefan Andersson-Engels. Design and validation of a fiber optic point probe instrument for therapy guidance and monitoring, Journal of Biomedical Optics 19 (7), 071408-071408 (2014)
- Haiyan Xie, Pontus Svenmarker, Johan Axelsson, Susanna Gräfe, Maria Kyriazi, Niels Bendsoe, Stefan Andersson-Engels and Katarina Svanberg. Pharmacokinetic and biodistribution study following systemic administration of Fospeg® – a Pegylated liposomal mTHPC formulation in a murine model. J Biophotonics, 8, 142–152 (2015).
- I. Bargigia, A. Nevin, A. Farina, A. Pifferi, C. D'Andrea, M. Karlsson, P. Lundin, G. Somesfalean and Sune Svanberg, Diffuse optical techniques applied to wood characterization. Journal of Near Infrared Spectroscopy, 21, 259–268 (2013).

- T. Svensson, E. Adolfsson, M. Burresi, R. Savo, C. Xu, D. S. Wiersma, S. Svanberg, Pore size assessment based on wall collision broadening of spectral lines of confined gas: experiments on strongly scattering nanoporous ceramics with fine-tuned pore sizes. Applied Physics B, 110, 147-154 (2013).
- P. Lundin, E. Krite Svanberg, L. Cocola, M. Lewander Xu, G. Somesfalean, S. Andersson-Engels, J. Jahr, V. Fellman, K. Svanberg, S. Svanberg. Noninvasive monitoring of gas in the lungs and intestines of newborn infants using diode lasers: feasibility study. J. Biomed. Opt. 18,, 127005 (2013).
- E. Krite Svanberg, P. Lundin, M. Larsson, J. Åkeson, K. Svanberg, S. Svanberg, S. Andersson-Engels and V. Fellman. Diode laser spectroscopy for non-invasive monitoring of oxygen in the lungs of newborn infants, Pediatric Research (in press).
-

6 Conference Proceedings

- D. Alfieri, S. Bacci, R. Cicchi, G. De Siena, V. Lotti, F.S. Pavone, R. Pini, F. Rossi, and F. Tatini, *Blue LED treatment of superficial abrasions*, Proceed. SPIE **8565**, 85650H (2013)
- D. Kapsokalyvas, V. Barygina, R. Cicchi, C. Fiorillo, and F.S. Pavone, *Evaluation of the oxidative stress of psoriatic fibroblasts based on spectral two-photon fluorescence lifetime imaging*, Proceed. SPIE **8588**, 85882D (2013)
- R. Cicchi, C. Matthaeus, T. Meyer, A. Lattermann, B. Dietzek, B.R. Brehm, J. Popp, and F.S. Pavone, *Characterization of Atherosclerotic Arterial Tissue using Multimodal Non-linear Optical Microscopy*, Proceed. SPIE **8797**, 87970D (2013)
- R. Cicchi, A. Cosci, S. Rossari, A. Sturiale, F. Giordano, V. De Giorgi, V. Maio, D. Massi, G. Nesi, A.M. Buccoliero, F. Tonelli, R. Guerrini, N. Pimpinelli, and F.S. Pavone, *A Combined Raman-Fluorescence Spectroscopic Probe for Tissue Diagnostics Applications*, Proceed. SPIE **8798**, 87980C (2013)
- F. Rossi, F. Tatini, R. Pini, S. Bacci, G. De Siena, R. Cicchi, F.S. Pavone, and D. Alfieri, *Improved Wound Healing in Blue LED Treated Superficial Abrasions*, Proceed. SPIE **8803**, 88030S (2013)
- R. Cicchi, F. Rossi, F. Tatini, S. Bacci, G. De Siena, D. Alfieri, R. Pini, and F. S. Pavone, *Irradiation with EMOLED improves the healing process in superficial skin wounds*, Proceed. SPIE **8926**, 892604 (2014)
- R. Cicchi, S. Anand, S. Rossari, A. Sturiale, F. Giordano, V. De Giorgi, V. Maio, D. Massi, G. Nesi, A. M. Buccoliero, F. Tonelli, R. Guerrini, N. Pimpinelli, and F. S. Pavone, *Multimodal fiber probe spectroscopy for tissue diagnostics applications: a combined Raman-fluorescence approach*, Proceed. SPIE **8939**, 89390U (2014)
- R. Cicchi, C. Matthäus, T. Meyer, A. Lattermann, B. Dietzek, B. R. Brehm, J. Popp, and F. S. Pavone, *Non-linear imaging and characterization of atherosclerotic arterial tissue using combined two photon fluorescence, second-harmonic generation and CARS microscopy*, Proceed. SPIE **8948**, 894807 (2014)
- A. Lihachev, I. Ferulova, J. Spigulis, M. Tamosiunas*. Simultaneous detection of tissue autofluorescence decay distribution and time-gated photo-bleaching rates*. Proc. SPIE 9504, 95040P (2015).
- I.Ferulova, A.Lihachev, J.Spigulis. *Fluorescence lifetime spectroscopy: potential for in-vivo estimation of skin fluorophores changes after low power laser treatment.* Proc. SPIE 9032, 90320B (2013).
- M Mousavi, H Xie, Z Xie, M Brydegaard, J Axelsson, S Andersson-Engels. Development of a novel combined fluorescence and reflectance spectroscopy system for guiding high-grade glioma resections: confirmation of capability in lab experiments, Proceedings of SPIE 9032M (2013).
- Z Xie, H Xie, M Mousavi, M Brydegaard, J Axelsson, S Andersson-Engels, Novel combined fluorescence/reflectance spectroscopy system for guiding brain tumor resections – hardware considerations. Proceedings of SPIE 90320R (2013).